Self-Consistent Nuclear Model*

BALAZS ROZSNYAI†‡
Department of Physics, University of California, Berkeley, California
(Received April 21, 1961; revised manuscript received July 10, 1961)

A Hamiltonian proposed by Duerr is applied to carry out self-consistent calculations for atomic nuclei. Average exchange forces, calculated from a plane-wave model, are included in the Hartree potential. In order to obtain agreement with the empirical data, two coupling constants and one constant representing the range of the interaction have to be adjusted. The range turns out to be 3.23×10^{-14} cm. Because this range is very short the calculations may not be justified and must be considered as a formal procedure. Having adjusted the three parameters, reasonable neutron and proton binding energies and nucleon densities are obtained for the nuclei O^{16}, Ca^{40}, Ce^{140}, and Pb^{208}.

I. INTRODUCTION

THE purpose of this paper is to present a simple nuclear model which mathematically leads to the self-consistent state of atomic nuclei.

Recently the Brueckner theory[1] achieved considerable success in explaining the properties of finite nuclei, although complete quantitative agreement has not been found as yet. Considering the difficulties of the formalism and the ambitious purpose of the theory this is not surprising.

The Brueckner theory has the disadvantage that its mathematical language is highly complex and thus presents great difficulties in actual computation. Therefore, it is of interest to make an attempt to solve the self-consistent problem in the framework of the much easier to handle independent-particle model. It has to be pointed out that the independent-particle model contains inherent inaccuracy, namely, the two-particle correlations are neglected. Since in case of short range forces they may be important the present paper should be regarded as a formal mathematical procedure.

We shall attempt to obtain a self-consistent single-particle potential using a Hamiltonian proposed by Duerr.[2] We limit ourselves to spherically symmetric fields and use as specific examples the nuclei Pb^{208}, Ce^{140}, Ca^{40}, and O^{16}. The Duerr-Hamiltonian looks as follows:

$$H=\sum_i \psi_i^* c\boldsymbol{\alpha}\cdot\mathbf{p}\psi_i+\beta Mc^2\sum_i\psi_i^*\psi_i-aMc^2\varphi\sum_i\psi_i^*\beta\psi_i$$
$$+bMc^2\varphi_0\sum_i\psi_i^*\psi_i+\frac{c^2}{2}[(\nabla\varphi)^2+\mu_1^2\varphi^2]$$
$$-\frac{c^2}{2}[(\nabla\varphi_0)^2+\mu_2^2\varphi_0^2], \quad (1.1)$$

where $\boldsymbol{\alpha}$ and β are the Dirac matrices, φ represents an attractive scalar field and φ_0 a repulsive field which transforms like the fourth component of a vector field, a and b are coupling constants. It was pointed out earlier in a paper by Johnson and Teller[3] that a pseudoscalar field gives zero average in the interior of a nucleus which is built up of shell model states. On the other hand this is not so in the case of a scalar field. Thus the Hamiltonian (1.1) is the most general type which gives nonzero average potential in the interior of a large nucleus. In the nonrelativistic limit both φ and φ_0 behave like scalars. As we shall see, it is necessary to have two fields because an attractive field alone yields a collapsed state. The Hamiltonian (1.1) represents a velocity dependent field because at high nucleon velocities the expectation value of β tends to zero. The effective velocity dependent potential is $Mc^2(-a\langle\beta\rangle\varphi+b\langle I\rangle\varphi_0)$ where I is the unit matrix.

Unfortunately the Duerr-Hamiltonian leads to wrong predictions for high-energy scattering. It has, however, the advantage that it gives a closed and handy formalism which leads to stable states of nuclei. Actually we shall attempt an approximation to a Hartree-Fock model by introducing the exclusion principle into the statistical formulation.

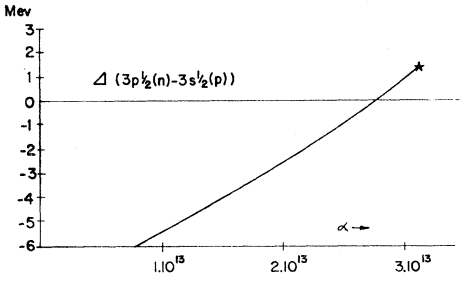

FIG. 1. Difference between the calculated last proton and last neutron binding energy in case of the Pb^{208} nucleus as a function of the range. The star means the experimental value.

II. DERIVATION OF THE SELF-CONSISTENT FORMALISM

In the nonrelativistic limit ($p\ll Mc$) the Hamiltonian (1.1) becomes after a Foldy-Wouthuysen transformation (see reference 2)

* Work supported in part by the U. S. Army Office of Ordnance Research and by the National Science Foundation.
† On the basis of a thesis submitted in partial fulfillment for the requirements of the Ph.D. degree at the University of California, Berkeley, California.
‡ Now at the IBM Product Development Laboratory, San Jose, California.
[1] K. A. Brueckner, A. M. Lockett, and M. Rotenberg, Phys. Rev. **121**, 255 (1961).
[2] Hans-Peter Duerr, Phys. Rev. **103**, 469 (1956).
[3] M. H. Johnson and E. Teller, Phys. Rev. **98**, 783 (1955).

$$H=\sum_i \psi_i^*\beta\Big\{\frac{1}{2Mg}\mathbf{p}^2-\frac{i\hbar}{2M^2c^2}(\nabla V/g^2)\cdot\mathbf{p}$$
$$-\frac{\hbar^2}{8M^2c^2}\nabla\cdot\Big[\frac{\nabla(V-V_0)}{g^2}\Big]\Big\}\psi_i$$
$$+\sum_i \psi_i^*\Big\{V_0-\beta V+\beta Mc^2$$
$$+\frac{\hbar^2}{4M^2c^2g^2}\frac{1}{r}\frac{d}{dr}(\beta V+V_0)(\boldsymbol{\sigma}\cdot\mathbf{l})\Big\}\psi_i$$
$$+\frac{1}{2a^2M^2c^2}[(\nabla V)^2+\mu_1^2V^2]$$
$$-\frac{1}{2b^2M^2c^2}[(\nabla V_0)^2+\mu_2^2V_0^2], \quad (2.1)$$

where

$$V=aMc^2\varphi; \quad V_0=bMc^2\varphi_0; \quad g=1-V/Mc^2.$$

It is tacitly assumed in (2.1) that the time derivatives $\partial V/\partial t$ and $\partial V_0/\partial t$ are zeros. We see that in the positive energy states ($\langle\beta\rangle=1$) there is a large spin-orbit interaction. In previous models this large spin-orbit interaction has been generally taken as a Thomas-type interaction in which a phenomenological factor occured.

Formula (2.1) is the Hamiltonian in the Hartree approximation.

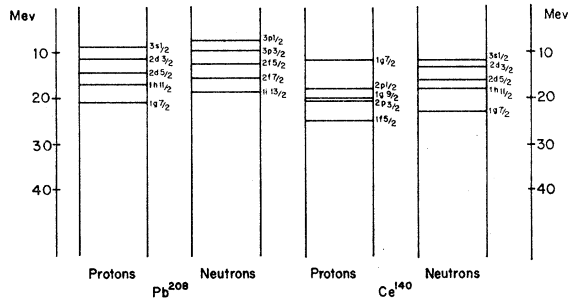

FIG. 2. Top energy levels in self-consistent fields. $\alpha=3.10\times10^{13}$ cm^{-1}, $g_1=2.3g\times10^{-8}$ cgs, $g_2=1.80\times10^{-8}$ cgs.

The Pauli exclusion principle requires that the total wave function of the N-particle system be antisymmetric which leads to the determinant form for the total wave function and to the Hartree-Fock equations for the single-particle functions. Instead of solving the complicated Hartree-Fock equations we try to modify the Hartree equations in such a way that these modified Hartree equations should yield approximately the same single-particle functions and energies as the correct Hartree-Fock equations. We can do that by introducing an exchange potential V_{ex} which results from the average exchange effects. We shall add this potential to the simple Hartree potentials to obtain the collective potential to be used in the modified Hartree approximation.

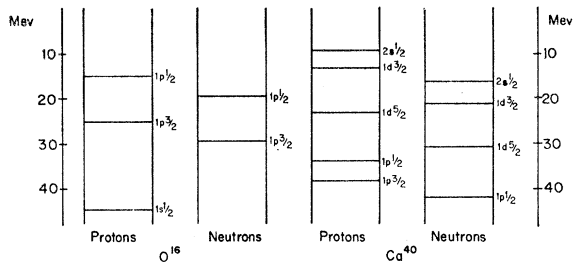

FIG. 3. Top energy levels in self-consistent fields. $\alpha=3.10\times10^{13}$ cm^{-1}, $g_1=2.3g\times10^{-8}$ cgs, $g_2=1.80\times10^{-8}$ cgs.

We assume that V_{ex} satisfies a Yukawa type equation

$$\nabla^2V_{ex}-\mu^2V_{ex}=-\frac{g^2\mu^2}{2\pi}f(\rho;\mu), \quad (2.2)$$

where $f(\rho;\mu)$ is given by (A1.9) in Appendix I. (For detailed discussion of the exchange potential see Appendix I.) We have to keep in mind that the exchange effect acts only between particles having the same spin and isotopic spin state. The proton and neutron distributions are in general different in a nucleus and the exchange potentials acting on them will be different as well.

Because of this difference between the proton and neutron exchange effects the effective meson potential acting on a single proton and neutron in a nucleus will be different. Since in most cases there are more neutrons than protons in a nucleus the meson well for protons will be deeper. This difference is counteracted by the Coulomb repulsion.

The inclusion of the Pauli principle in the above discussed way yields the total Hamiltonian for a system

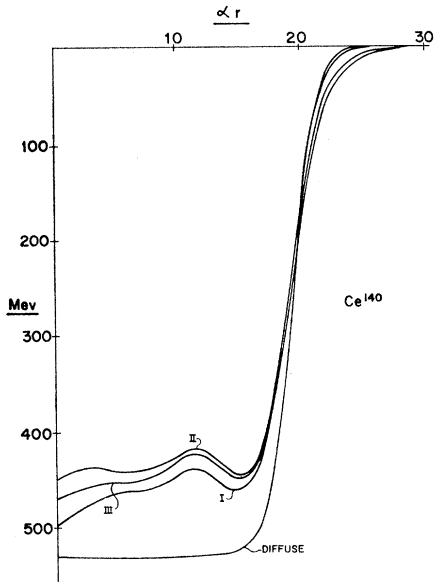

FIG. 4. The "big" scalar potential for protons (V_p) in the Ce^{140} nucleus belonging to different iterations.

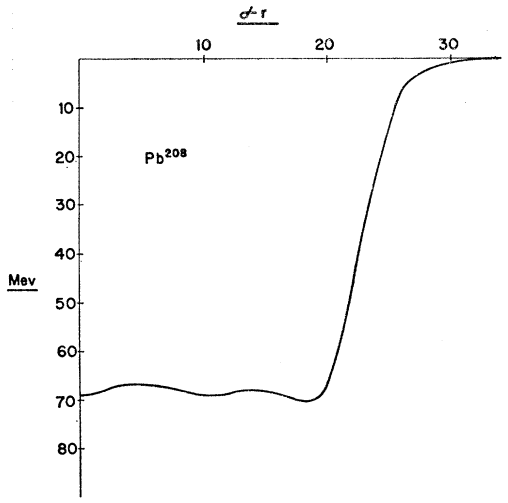

FIG. 5. Self-consistent neutron potential (V_n-V_{n0}) for the Pb^{208} nucleus.

consisting of Z protons and N neutrons

$$H=\sum_{i=1}^{Z}H_{pi}+\sum_{i=1}^{N}H_{ni}+H_{\text{scalar meson}}+H_{\text{vector meson}}. \quad (2.3)$$

Here the Hamiltonian for a single proton is

$$H_{pi}=\psi_i^*\Big\{\frac{1}{2M(1-V_p/Mc^2)}\mathbf{p}^2-\frac{i\hbar}{2M^2c^2}\frac{\nabla V_p}{(1-V_p/Mc^2)^2}\cdot\mathbf{p}$$
$$-\frac{\hbar^2}{8M^2c^2}\nabla\cdot\left(\frac{\nabla(V_p-V_{p0})}{(1-V_p/Mc^2)^2}\right)+Mc^2-(V_p-V_{p0})$$
$$+\Big[\frac{\hbar^2}{4M^2c^2}\left(\frac{1}{(1-V_p/Mc^2)^2}\frac{1}{r}\frac{d}{dr}(V_p+V_{p0})\right.$$
$$\left.-\frac{1}{r}\frac{dV_c}{dr}\right)\times\epsilon\Big]+V_c\Big\}\psi_i, \quad (2.4)$$

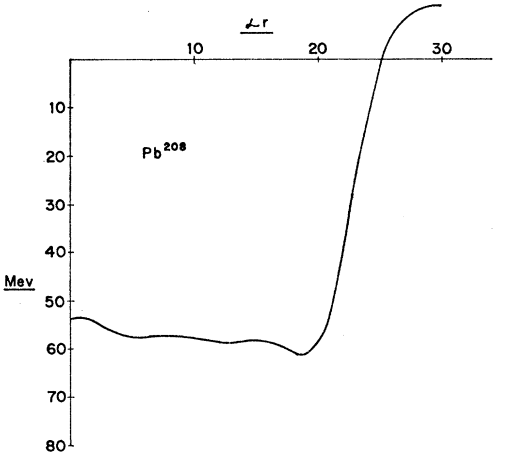

FIG. 6. Self-consistent proton potential ($V_p-V_{p0}-V_c$) for the Pb^{208} nucleus.

where $\epsilon=l$ for $j=l+\frac{1}{2}$, $\epsilon=-l-1$ for $j=l-\frac{1}{2}$. The last two terms in (2.4) are the spin-orbit interaction and the Coulomb repulsion V_c. The two collective meson potentials for protons V_p and V_{p0} correspond to V and V_0 in the formula (2.1), and they are given by

$$V_p=V-V_{\text{ex}} \text{ for protons,}$$
$$V_{p0}=V_0-V_{0\,\text{ex}} \text{ for protons.}$$

Similarly the collective neutron potentials are

$$V_n=V-V_{\text{ex}} \text{ for neutrons,}$$
$$V_{n0}=V_0-V_{0\,\text{ex}} \text{ for neutrons.}$$

In the single-particle Hamiltonian for neutrons V_c is obviously omitted.

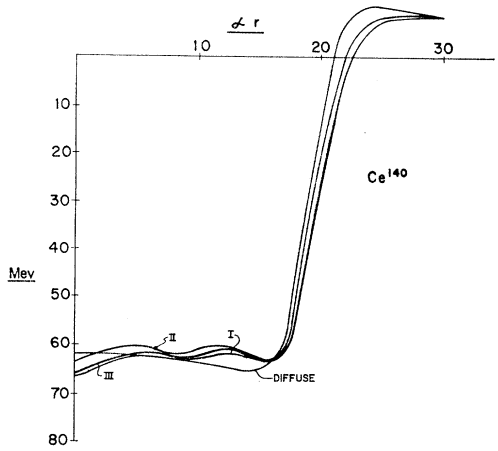

FIG. 7. Proton potentials ($V_p-V_{p0}-V_c$) for the Ce^{140} nucleus belonging to different iterations. For starting potential the diffuse type $V=D/[1+\exp\alpha(r-R)]$ was used. III can be considered as the self-consistent potential.

The Hamiltonian (2.3) combined with (2.2) for the exchange part yields the field equations for the collective potentials and the single-particle equations as well:

$$\nabla^2V_p-\mu_1^2V_p=-4\pi g_1^2\{\rho_p[1-K\rho_p^{\frac{2}{3}}/M^2c^2g_p^2]$$
$$+\rho_n[1-K\rho_n^{\frac{2}{3}}/M^2c^2g_n^2]$$
$$-(\mu_1^2/8\pi)f(\rho_p;\mu_1)\}, \quad (2.5)$$

$$\nabla^2V_{p0}-\mu_2^2V_{p0}=-4\pi g_2^2\{\rho_p+\rho_n$$
$$-(\mu_2^2/8\pi)f(\rho_p;\mu_2)\}, \quad (2.6)$$

$$H_p\psi_i=E_i\psi_i. \quad (2.7)$$

In (2.5) and (2.6),

$$\rho_p=\sum_{i=1}^{Z}|\psi_i|^2;\quad \rho_n=\sum_{i=1}^{N}|\psi_i|^2;$$

$$g_p=1-V_p/Mc^2;\quad g_n=1-V_n/Mc^2;$$

$$K=(3/10M)(3\pi^2)^{\frac{2}{3}}\hbar^2.$$

We redefine the coupling constants in a more familiar

way,

$$a^2M^2c^2=4\pi g_1^2; \quad b^2M^2c^2=4\pi g_2^2.$$

In (2.5) we used the approximation

$$\frac{\hbar^2}{2M}\sum_{i=1}^{z}\psi_i^*\nabla^2\psi_i\approx K\rho_p^{5/3},$$

which is good only in the case where the wave functions can be represented by plane waves.

The equations for the collective neutron potentials can be obtained in the same way, the only difference is that we have there $f(\rho_n;\mu)$. Finally the Coulomb potential V_c is determined by the Laplace equation

$$\nabla^2V_c=4\pi e^2\rho_p, \tag{2.8}$$

where e means the elementary charge (4.8024×10^{-10} cgs).

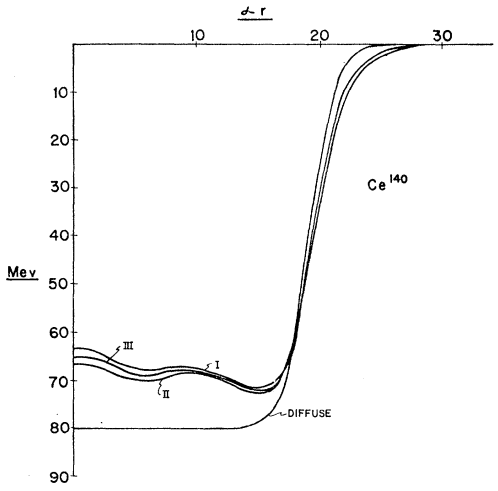

FIG. 8. Neutron potentials (V_n-V_{n0}) for the Ce^{140} nucleus belonging to different iterations. For starting potential the diffuse type $V=D/[1+\exp\alpha(r-R)]$ was used. III can be considered as the self-consistent potential.

We observe that the repulsion which eventually keeps the nucleus at a finite size appears both in the single-particle Hamiltonian (2.4) and in the equation for the attractive potential (2.5). In (2.4) it appears in the form of an increased kinetic energy because of the effective mass

$$M_p^*=M(1-V_p/Mc^2).$$

We also see from (2.5) that in case of high momenta the attractive potential becomes small whereas the repulsive part in (2.6) remains large. This latter effect corresponds to the relativistic case where βV tends to zero with increasing momenta.

III. DISCUSSION OF THE RESULTS

The Eqs. (2.5)–(2.7) form the basis for the self-consistent calculations which were carried out for the

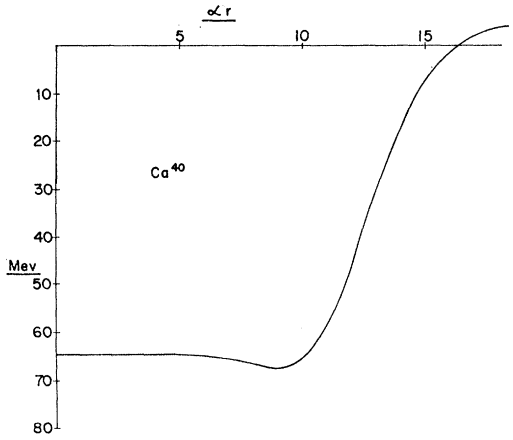

FIG. 9. Self-consistent proton potential ($V_p-V_{p0}-V_c$) for the Ca^{40} nucleus.

O^{16}, Ca^{40}, Ce^{140}, and Pb^{208} nuclei. Since we do not assume that the two-particle interaction is represented by the exchange of single π mesons, the Compton wavelength of the fields V and V_0 was taken as a free parameter. We shall call it briefly the range of the potentials. The range of V and V_0 has to be taken as equal. Otherwise the effective potential $V-V_0$ oscillates at the nuclear surface. The nuclear radius, or in other words r_0 in the nuclear radius expression $R=r_0A^{\frac{1}{3}}$ is known from the experiments with limited accuracy. According to these r_0 is likely to be between 1.2 and 1.4×10^{-13} cm. The nuclear size, the binding energy of the last neutron and proton can be reproduced by varying three parameters which are the range of the potentials and the coupling constants g_1 and g_2. The ratio of the last proton and last neutron binding energies is a function mainly of the range. The calculations for the Pb^{208} nucleus were carried out with several ranges and it was found that the correct last proton and last neutron binding ratio was reproduced by taking $\alpha=3.10\times10^{13}$ cm^{-1} ($\alpha=\mu_1=\mu_2$).

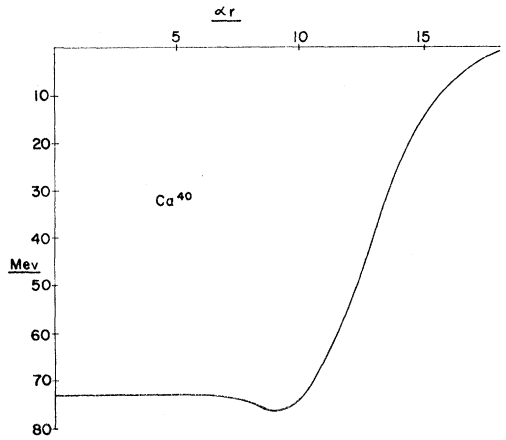

FIG. 10. Self-consistent neutron potential (V_n-V_{n0}) for the Ca^{40} nucleus.

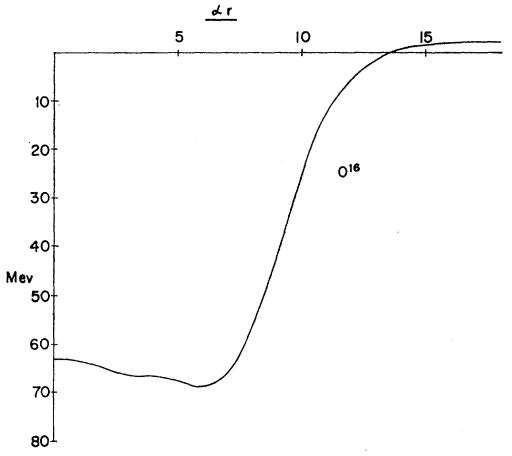

FIG. 11. Self-consistent proton potential ($V_p - V_{p0} - V_c$) for the O^{16} nucleus.

A. Self-Consistency

The self-consistent state was obtained usually after the third or fourth iteration regardless of the range of the potentials. For starting potentials the diffuse type $V=D/[1+\exp\alpha(r-R)]$ was used, where the potential depths had to be chosen adequately. As mentioned above the correct β^+ and β^- stabilities for the neighboring nuclei of the Pb^{208} nucleus were reproduced with a potential range $1/\alpha=3.23\times10^{-14}$ cm (see Fig. 1). This short range was needed in order to produce a sufficiently great difference between the interactions of like and unlike nucleons. The small value of the range raises serious doubt as to the validity of the use of average potentials. Actually the exchange forces are substitutes for the more usual symmetry forces. It is possible that the former results of our calculations correspond to a physical situation in which the range is longer and symmetry forces are added.

B. Top Levels

The correctness of the top level system can be checked from the experimentally known (γ,n) threshold energies and from the β^+ and β^- decay energies and angular momentum states of the neighboring nuclei.

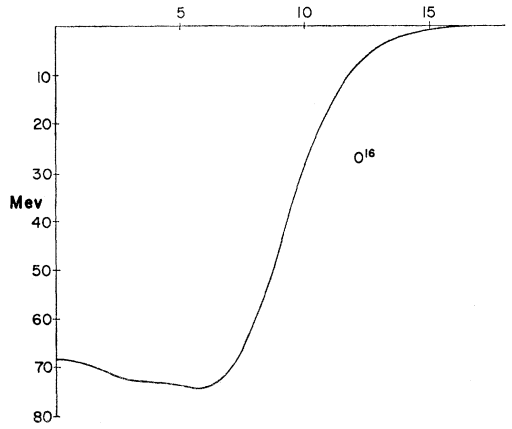

FIG. 12. Self-consistent neutron potential ($V_n - V_{n0}$) for the O^{16} nucleus.

The stability of the Pb^{207} nucleus and the activity of AcC''^{207} with 1.47-Mev β^- energy indicates that in the case of Pb^{208} nucleus we can expect the top neutron level ($3p_{\frac{1}{2}}$) to be about 1.47 Mev higher than the top proton level ($3s_{\frac{1}{2}}$). The coupling constants were adjusted to reproduce the nuclear radius and the experimentally measured (γ,n) threshold energy for the top neutron level, which in the case of the Pb^{208} nucleus is 7.4 Mev. The sequence of the top proton and neutron levels can be checked by the angular momentum states of the neighboring odd Z and odd N nuclei, respectively. As we go away from the magic shells we go from the spherically symmetric state to the deformed core state, consequently our level system which was calculated in spherically symmetric fields cannot be trusted quantitatively. Nevertheless, the Tl^{205}, Tl^{203}, Au^{197} nuclei confirm that the $3s_{\frac{1}{2}}$ and $2d_{\frac{3}{2}}$ levels are the top proton levels, similarly the Pb^{207} and Hg^{201} nuclei show the $3p_{\frac{1}{2}}$ and $3p_{\frac{3}{2}}$ levels as top neutron levels.

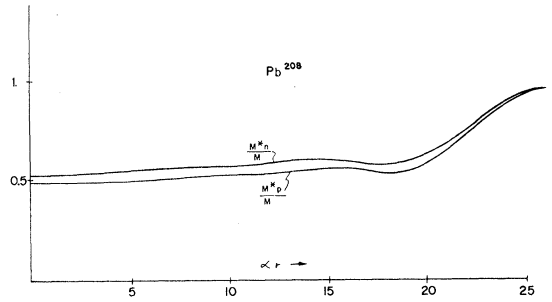

FIG. 13. Effective nucleon mass in the self-consistent field of the Pb^{208} nucleus. $\alpha=3.10\times10^{13}$ cm^{-1}.

The above discussions seem to indicate that the parameter set $\alpha=3.10\times10^{13}$ cm^{-1}, $g_1=2.39\times10^{-8}$ cgs, $g_2=1.80\times10^{-8}$ cgs yields the self-consistent state for the Pb^{208} nucleus and predicts top levels for the neighboring nuclei with fairly good accuracy (see Fig. 2). We may observe that the magnitude of the coupling constants are enormous, $g_1^2/\hbar c\sim18$, $g_2^2/\hbar c\sim10$. This is the result of the short range interaction alone. Taking the range as a variable the same magnitude for the potential depth can be obtained by keeping g/α constant. Thus the π meson range would result $g_1^2/\hbar c\sim0.95$, $g_2^2/\hbar c\sim0.53$.

TABLE I. Comparison of calculated and experimental neutron separation energies.

Nucleus	(γ,n) threshold (Mev)[a]	Last neutron binding (Fig. 1–2)
O^{16}	16.3 ±0.4	19.25
Ca^{40}	15.9 ±0.4	16.25
Ce^{140}	9.05±0.2	11.5
Pb^{208}	7.4 ±0.1	7.4

[a] Taken from: *Experimental Nuclear Physics*, edited by E. Segrè (John Wiley & Sons, Inc., New York, 1953), Vol. II.

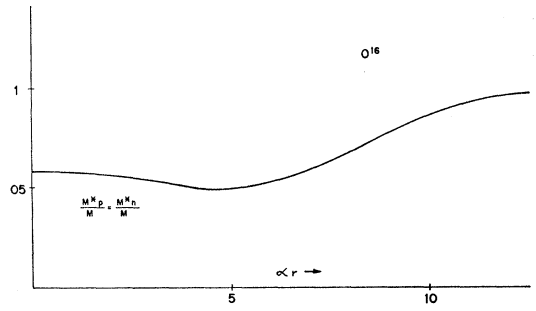

FIG. 14. Effective nucleon mass in the self-consistent field of the O^{16} nucleus. $\alpha=3.10\times10^{13}$ cm^{-1}.

This range however does not give the empirical β^+ and β^- stabilities.

Having fixed these parameters for the Pb^{208} nucleus the calculations were carried out for the Ce^{140}, Ca^{40} and O^{16} nuclei. Table I shows that the obtained last neutron binding energies are in close agreement with the experimental (γ,n) threshold energies.

The stable La^{139} nucleus with $J=\frac{7}{2}$ and the unstable Ce^{139} nucleus which transforms with K capture to La^{139} indicate that the top proton level is about 0.5 Mev higher than the top neutron level in the case of the Ce^{140} nucleus (see Fig. 2). The O^{16} and Ca^{40} nuclei have equal numbers of protons and neutrons, consequently the top proton level must be considerably higher than the top neutron level (see Fig. 3). This is proved by the short half-life of β^+-unstable O^{15} and Ca^{39} nuclei.

There is one remarkable difference between the level system shown in Figs. 2 and 3 and the empirical data. The $1d_{\frac{3}{2}}$ level has to be above the $2s_{\frac{1}{2}}$ level both in the proton and neutron case, and similarly the $2d_{\frac{3}{2}}$ level is above the $3s_{\frac{1}{2}}$ level for neutrons. (The only case where the $3s_{\frac{1}{2}}$ level is above the $2d_{\frac{3}{2}}$ level happens in the proton case in accordance with the level system of Pb^{208}.) The reason for this discrepancy lies partly in the inaccurate way of calculating the exchange effect. The average exchange effect has been calculated assuming for the wave functions plane waves. This is a good approximation for

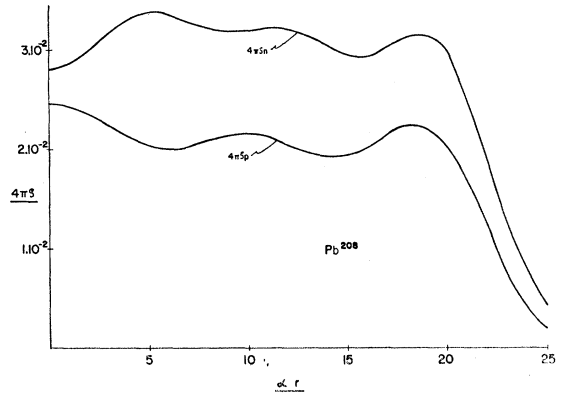

FIG. 15. Proton and neutron densities in the Pb^{208} nucleus.

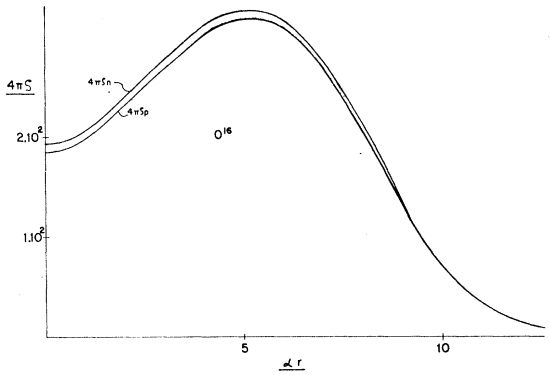

FIG. 16. Proton and neutron densities in the O^{16} nucleus.

heavy nuclei as in the case of Pb^{208}; however for light nuclei it is inaccurate. Furthermore, the exchange effects are different for different nucleon states and we calculated the exchange potential in an average way.

IV. CONCLUSION

We saw that the Hamiltonian (1.1) in Sec. I yields saturation and it also has the nice property that it automatically gives a large spin-orbit interaction. However, this Hamiltonian predicts wrong nucleon-nucleus scattering data at high energies. In case of high energies it predicts a net repulsion which is in contradiction with the experiments. On the other hand, at low energies as in the ground state of the nucleus it works surprisingly well.

The magnitude of the coupling constants g_1 and g_2 had to be chosen in such a way that there should be enough repulsion to produce the right nuclear radii and that, furthermore, the depth of the effective potential $V-V_0$ should give the correct binding energy for the top neutron. The result is that the potentials V and V_0 have the order of magnitude 450 and 390 Mev, respectively

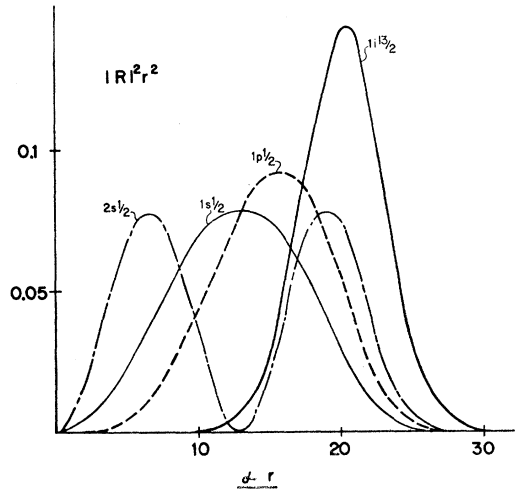

FIG. 17. Single-particle radial distributions in the Pb^{208} nucleus. R is the radial part of the single particle wave function.

(see Fig. 4); therefore, the effective potential is the net difference of the two nearly canceling fields (see Figs. 5–12). Thus, our model is a rather drastic device which keeps the nucleus at a finite size. What really matters is the velocity dependent difference between the large potentials. It can be expected that any velocity dependent potential of similar strength, such as following from the Brueckner theory, would give similar results. One of the consequences of the model is that the nucleons inside the nucleus have an effective mass of the magnitude 0.5 times the bare mass (see Figs. 13 and 14). Figures 15 and 16 represent the density profile of the Pb^{208} and O^{16} nuclei, respectively. We may notice that in case of equal number of protons and neutrons as in the case of O^{16} the Coulomb repulsion pushes the protons somewhat outward. Figure 17 shows the radial part of some wave functions for the Pb^{208} nucleus.

The scalar field corresponding to the range that we found might be represented by mesons having the mass 4.43 times the mass of the π meson. This is in the range of a K-meson Compton-wavelength. The range, however, can not be established accurately by our calculations, and its physical reality is doubtful.

It is of some interest that by the use of three adjustable parameters a wide variety of nuclear binding energies and levels could be reproduced within limited errors.

ACKNOWLEDGMENTS

The author is very much indebted to Dr. Edward Teller for the many helpful discussions and suggestions throughout this work. Thanks are due to Dr. Harry Schey of the University of California Lawrence Radiation Laboratory for the many discussions and for his assistance throughout the calculations. Thanks are also due to Dr. Peter Redmond who checked some of the difficult details of the calculations.

APPENDIX

I. Exchange Potential in a Nucleon Gas

In this section we calculate the exchange energy of a nucleon having the wave vector $\mathbf{k}$ moving in a nucleon gas. We assume that the wave functions can be represented by plane waves. This is a fairly good approximation for heavy nuclei. We also assume a Yukawa type interaction between two particles,

$$V(1,2)=-g^2[\exp(-\alpha|\mathbf{r}_1-\mathbf{r}_2|)]/(|\mathbf{r}_1-\mathbf{r}_2|). \quad \text{(A1.1)}$$

Let us calculate first the exchange term between two particles:

$$A_{jl}=-\int\int \rho_{jl}(\mathbf{r}_1)\rho_{jl}^*(\mathbf{r}_2)V(1,2)dv_1dv_2, \quad \text{(A1.2)}$$

where $\rho_{jl}(\mathbf{r})=\psi_j(\mathbf{r})\psi_l^*(\mathbf{r})$. Using (A1.1) for A(1.2) we have

$$A_{jl}=\int \rho_{jl}(\mathbf{r}_1)V_{jl}(\mathbf{r}_1)dv_1, \quad \text{(A1.3)}$$

where

$$V_{jl}(\mathbf{r}_1)=g^2\int \rho_{jl}^*(\mathbf{r}_2)[\exp(-\alpha|\mathbf{r}_1-\mathbf{r}_2|)]/(|\mathbf{r}_1-\mathbf{r}_2|)dv_2.$$

$V_{jl}(\mathbf{r})$ also satisfies the differential equation

$$\nabla^2V_{jl}-\alpha^2V_{jl}=-4\pi g^2\rho_{jl}^*. \quad \text{(A1.4)}$$

Using plane waves we have

$$\rho_{jl}^*(\mathbf{r})=(1/\Omega)\exp[-i(\mathbf{k}_j-\mathbf{k}_l)\cdot\mathbf{r}].$$
$$(\Omega=\text{volume occupied.})$$

The solution of (A1.4) is given by

$$V_{jl}(\mathbf{r})=[(4\pi g^2)/(\alpha^2+|\mathbf{k}_j-\mathbf{k}_l|^2)]\rho_{jl}^*(\mathbf{r}). \quad \text{(A1.5)}$$

Replacing (A1.5) into (A1.3) we obtain

$$A_{jl}=4\pi g^2\Omega^{-1}/(\alpha^2+|\mathbf{k}_j-\mathbf{k}_l|^2). \quad \text{(A1.6)}$$

Formula (A1.6) gives the exchange energy of two nucleons. The total exchange energy of a nucleon having a momentum $\hbar\mathbf{k}_j$ in a nucleon gas is given by

$$V_{ex}=4\pi g^2\Omega^{-1}\int_0^N(\alpha^2+|\mathbf{k}_j-\mathbf{k}_l|^2)^{-1}dn;$$
$$dn=(1/4\pi^2)\Omega k_l^2dk_ld(\cos\vartheta),$$

thus

$$V_{ex}=(g^2/\pi)\int_0^{K_{max}}\int_{-1}^{+1}(\alpha^2+k_j^2+k_l^2+2k_jk_l\cos\vartheta)^{-1}\times k_l^2dk_ld(\cos\vartheta)$$
$$=(g^2/2\pi)\int_0^{K_{max}}k_j^{-1}\ln\frac{\alpha^2+(k_j+k_l)^2}{\alpha^2+(k_j-k_l)^2}k_ldk_l. \quad \text{(A1.7)}$$

The integral in (A1.7) can be carried out in a long but straightforward way and it yields

$$V_{ex}=\left(\frac{g^2}{2\pi}\right)\left\{\left(\frac{1}{2k_j}\right)(K_{max}^2-k_j^2+\alpha^2)\ln\frac{(K_{max}+k_j)^2+\alpha^2}{(K_{max}-k_j)^2+\alpha^2}\right.$$
$$+2K_{max}-2\alpha\tan^{-1}\frac{K_{max}+k_j}{\alpha}$$
$$\left.-2\alpha\tan^{-1}\frac{K_{max}-k_j}{\alpha}\right\}. \quad \text{(A1.8)}$$

Formula (A1.8) gives the exchange energy of one nucleon with all the nucleons in a nucleon gas. It contains the self-exchange energy too which in the Hartree-Fock method cancels the self energy appearing in the Hartree method. We see from (A1.8) that the exchange potential depends on the momentum $\hbar k_j$ of the nucleon in question. For a nucleon having the average mo-

mentum $\frac{3}{4}K_{\max}$ (A1.8) yields

$$V_{ex}=\left(\frac{g^2}{2\pi}\right)\left\{\left(\frac{2}{3}\right)(3\pi^2\rho)^{-\frac{1}{3}}\left[\left(\frac{7}{16}\right)(3\pi^2\rho)^{\frac{2}{3}}+\alpha^2\right]\times\ln\frac{49(3\pi^2\rho)^{\frac{2}{3}}+16\alpha^2}{(3\pi^2\rho)^{\frac{2}{3}}+16\alpha^2}+2(3\pi^2\rho)^{\frac{1}{3}}-2\alpha\tan^{-1}[(7/4)(3\pi^2\rho)^{\frac{1}{3}}\alpha^{-1}]-2\alpha\tan^{-1}[(1/4)(3\pi^2\rho)^{\frac{1}{3}}\alpha^{-1}]\right\}. \quad \text{(A1.9)}$$

In (A1.9) we used the relation $K_{\max}=(3\pi^2\rho)^{\frac{1}{3}}$, where ρ is the nucleon density. It is assumed that half of the nucleons are in the state spin up and half of them in spin down.

Formula (A1.9) is valid for an infinitely large nucleus. In that case, the potential energy is a function of the nucleon density alone, which is a constant. In analogy with the equation which holds for the classical type direct potential we assume that for finite size nuclei the exchange potential also satisfies a Yukawa type equation

$$\nabla^2V_{ex}-\alpha^2V_{ex}=-(g^2\alpha^2/2\pi)f(\rho;\alpha), \quad \text{(A1.10)}$$

where $f(\rho;\alpha)$ is the expression in the parenthesis on the right side of (A1.9). We observe that in the interior of the nucleus where ∇^2V_{ex} can be neglected formula (A1.10) goes over to (A1.9). Near the surface the term ∇^2V_{ex} becomes important. No justification of this term is known to us beyond the statements that a surface term of this order of magnitude is reasonable and that the introduction of this term greatly simplifies the treatment of the expression for V_ρ and V_{p0} in Sec. II.

II. Computational Methods

The equation for the radial part of the wave function has the form

$$R''+f(x)R'+[k_{njl}(x)-\lambda_{njl}g(x)]R=0, \quad \text{(A2.1)}$$

where the functions $f(x)$ and $k(x)$ contain the potentials and spin-orbit term, $g(x)$ is the effective mass function defined in Sec. II, and λ_{njl} is the eigenvalue in dimensionless units.

(A2.1) was solved step by step using the approximation

$$R'(x)\sim[R(x+\Delta x)-R(x-\Delta x)]/2\Delta x,$$
$$R''(x)\sim[R(x+\Delta x)-2R(x)+R(x-\Delta x)]/(\Delta x)^2.$$

The solution of the field Eqs. (2.5) and (2.6) was performed by simple integration[4] using the Weddle numerical integration method.

The IBM 704 electronic computer was programmed to solve (A2.1) and the field equations and the solutions were carried out until the self-consistent state was reached.

[4] For details see R. Mises: *Differential and Integral Gleichungen der Mechanik and Physik* (Friedrich Vieweg und Sohn, Braunschweig, 1930), Vol. 1.